IET Communications

Research Article

Multiple-input–multiple-output cooperative spatial modulation systems

ISSN 1751-8628
Received on 28th August 2016
Revised 19th June 2017
Accepted on 17th July 2017
E-First on 13th October 2017
doi: 10.1049/iet-com.2016.0977
www.ietdl.org

Gökhan Altın[1] ✉, Ümit Aygölü[1], Ertugrul Basar[1], Mehmet E. Çelebi[1]

[1]Department of Electronics and Communication Engineering, Istanbul Technical University, 34469 Istanbul, Turkey

✉ *E-mail: alting@itu.edu.tr*

Abstract: In this study, the authors propose novel cooperative spatial modulation (SM) systems with two main relaying techniques [amplify-and-forward (AF) and decode-and-forward (DF)], where all nodes have multiple transmit and/or receive antennas. Most of the studies in the literature of cooperative SM systems, which combine the advantages of cooperative communications and SM systems, consider only the space shift keying (SK) scheme with single receive/transmit antenna at relay and destination. Since the error performance of SM highly depends on the number of receive antennas and more flexible cooperative communications systems can be obtained by using SM with multiple antennas, it is essential to investigate multi-antenna cooperative SM systems. They derive analytical expressions of the average bit error probability for both the newly proposed cooperative SM-DF and cooperative SM-AF systems and validate with the computer simulation results. Furthermore, they present the bit error rate comparison of considered systems with classical *M*-ary phase SK/quadrature amplitude modulation cooperative systems. Computer simulation results indicate that multiple antennas cooperative SM systems provide better error performance than classical cooperative systems for both relaying techniques.

1 Introduction

Spatial modulation (SM) [1] is an alternative method to classical multiple-input– multiple-output (MIMO) transmission techniques such as vertical-Bell Labs layered space–time and space–time block codes (STBCs) [2, 3]. In SM, the information is transmitted via the conventional amplitude-phase modulation (APM) symbols along with the active antenna indices. $\log_2(N_t)$ bits are mapped to the index of activated transmit antenna and $\log_2(M)$ bits are allocated for the APM, where N_t is the number of transmit antennas and M is the constellation size. Hence, the total number of transmitted bits becomes $\log_2(N_tM)$ for the SM scheme. Since only one transmit antenna is active during the transmission, one radio frequency chain is sufficient at the transmitter of SM, and additionally inter-channel interference is eliminated. Space shift keying (SSK) is a special case of SM, where the information is transmitted through only transmit antenna indices [4]. SSK systems are relatively simple; however, their data rate is lower compared with SM for the same number of transmit antennas. SM techniques have attracted considerable attention from researchers in the past few years and have been considered as potential candidates for next generation wireless networks [5].

Cooperative communications which provide effective ways to combat fading has been investigated extensively during the recent times. Two main relay processing techniques are commonly used: decode-and-forward (DF) and amplify-and-forward (AF) relaying [6]. In the former, the relay (*R)* decodes the incoming signal and forwards the newly encoded data to the destination (*D*). In the latter, *R* only amplifies and retransmits the received signal.

The advantages of SM and cooperative communication systems have been combined in [7–18]. In [7], a special cooperative communications scenario called dual-hop system, where there is no direct link between source (*S*) and destination (*D*), is considered. In this dual-hop SM system, all nodes have multiple antennas and *R* uses DF strategy. In [8], bit error rate (BER) performance of a dual-hop SSK system applying AF relaying is investigated for single receive antenna at both *R* and *D*. A classical cooperative communications scenario is considered in [9], where *S* transmits its data using SSK to *N* relays and *D* (all nodes have single transmit and receive antennas) in the first time slot. In the following *N* time slots, *N* relays successively forward the incoming signal with one of the relay processing techniques, where both AF and DF strategies are investigated. Since the relays have single antenna, communication between *R* and *D* cannot be performed with SSK in DF systems. In [10], the dual-hop SSK system in [8] is enhanced to an *N*-relay system using opportunistic relaying to increase the spectral efficiency. Cooperative SM system with multi-antenna *S*, single transmit/receive antenna, multiple-*R* using DF strategy and single receive antenna *D* is considered in [11]. The first cooperative system in which all nodes have multiple transmit and receive antennas is introduced in [12]. However, the exact BER analysis for SSK-DF system with incremental relaying and selection combining at *D* is derived only for two transmit antennas at *S* and *R*.

Combining the advantages of both SM and STBC, the STBC-SM scheme is introduced in [13]. Applying the idea of STBC-SM to the cooperative systems is investigated in [14], where end-to-end pairwise error probability (PEP) analysis and optimal source–relay power allocation is presented.

Furthermore, the outage probability analysis of cooperative SM systems can be found in [15] and the combination of SM/SSK and physical layer network coding (PLNC) is performed in [16–18]. Since a framework for PLNC is the cooperative system, our study can be the precursor for PLNC-SM systems. PLNC is proposed to increase the spectral efficiency of cooperative communications, where different users share the same relay to communicate with each other at the same time.

In this work, we propose novel cooperative SM systems with AF and DF techniques, where all nodes have multiple transmit and/or receive antennas, an issue which has not been studied before. The previous studies in the literature of cooperative SM systems generally consider the SSK technique instead of SM. Additionally, most of these studies assume single transmit and/or receive antenna at the relay(s) and destination. As known, the SM/SSK schemes need at least two transmit antennas to map information bits to the antenna indices. Furthermore, a cooperative SM system with DF relaying, where the relay(s) has only one transmit antenna is not a complete SM system since the relay(s) cannot re-encode the decoded data into the SM symbols. Moreover, to improve the error performance compared with APM, an SM system requires at least two receive antennas. To the best of our knowledge, a comprehensive work on cooperative SM systems that

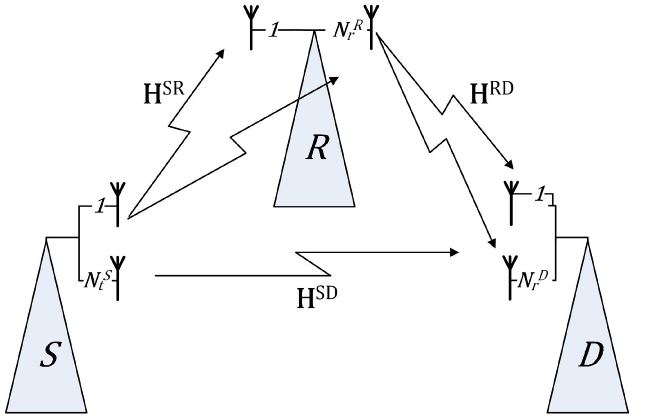

Fig. 1 *Cooperative communications scenario with SM MIMO-DF*

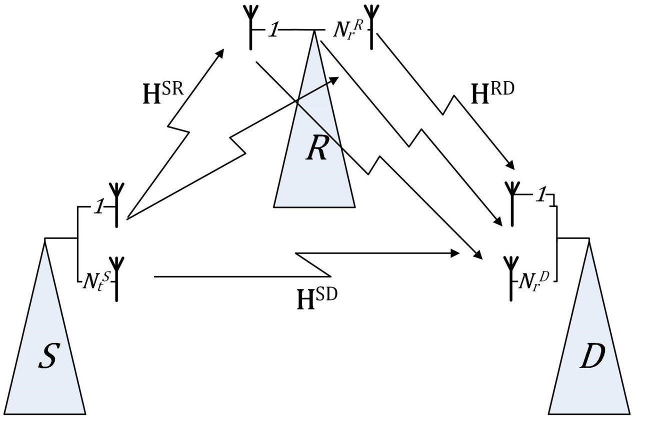

Fig. 2 *MIMO-AF configuration ($N_t^R = N_r^R = N^R$)*

have multiple transmit and/or receive antennas at *R* and *D* has not been performed in the literature yet.

We consider a cooperative SM scheme where *S*, *R and* *D* have multiple transmit/receive antennas. In this scheme, *S* sends the SM symbols to *R* and *D* in the first phase. In the second phase, *R* processes and forwards the received signal either by amplifying or decoding. When it uses the AF strategy, it only amplifies the received signal at each antenna and sends it from all antennas (MIMO-AF). When DF strategy is utilised, *R* decodes the received signal using maximum-likelihood (ML) detection and maps the estimated signal to a new SM symbol and forwards it to *D* in the second phase (MIMO-DF). At *D*, ML detection is employed to determine the transmitted SM symbol.

In this paper, we derive the average bit EPs (ABEP) for both the MIMO-AF and the MIMO-DF systems and validate them with the computer simulations results. Furthermore, these two cooperative SM systems are compared with the classical cooperative systems [6] using *M*-ary modulations in terms of BER performance. Computer simulations and analytical expressions show that the proposed MIMO-DF and MIMO-AF systems provide considerable error performance improvements over conventional cooperative APM systems. Finally, the BER comparison of MIMO-AF and MIMO-DF cooperative SM systems are presented.

The rest of this paper is organised as follows. In Section 2, the system model is given. In Sections 3 and 4, the ABEP analysis of cooperative SM system with DF and AF relaying are given, respectively. The theoretical and computer simulation results are presented in Section 5. Finally, Section 6 concludes this paper.

Notations: A scalar, a vector and a matrix will, respectively, be denoted by a lower-/upper-case italic, a lower-case boldface and an upper-case boldface letter. $(\cdot)^{\mathrm{T}}$, $(\cdot)^{\mathrm{H}}$ and $\|\cdot\|$ represent transpose, Hermitian transpose and Euclidean/Frobenius norm of a vector/matrix, respectively. $\mathbb{C}^{m\times n}$ represents the dimensions of a complex-valued matrix. $\Pr\{\cdot\}$ denotes the probability of an event and $E\{\cdot\}$ is the expectation operation. The probability density function (pdf) and the cumulative distribution function of a random variable (rv) X are given as $f_X(x)$ and $F_X(x)$, respectively. $\mathscr{C}\mathscr{N}(0,\sigma^2)$ denotes the circularly symmetric zero-mean complex Gaussian distribution with variance σ^2 and $\boldsymbol{I}_M$ is the identity matrix with dimensions $M\times M$. Gamma(α,β) denotes the Gamma distribution with shape and scale parameters α and β, respectively. $Q(\cdot)$ is the tail probability of standard Gaussian distribution and $\binom{\cdot}{\cdot}$ denotes the binomial coefficient. $\Gamma(\cdot)$ is the gamma function. $M_\gamma(s) = E\{\mathrm{e}^{s\gamma}\}$ is the moment generating function (MGF) of a rv γ and $\mathrm{tr}(\cdot)$ is the trace operator.

2 System model

The considered cooperative communications system for SM MIMO-DF and MIMO-AF consisting of a single relay is given in Figs. 1 and 2. In these systems, *S* and *R* have N_t^{S} and N_t^{R} transmit antennas, whereas *R* and *D* have N_r^{R} and N_r^{D} receive antennas, respectively. The channel matrices composed of channel fading coefficients between *S*–*R*, *S*–*D* and *R*–*D* can be given as $\boldsymbol{H}^{SR}\in\mathbb{C}^{N_r^{\mathrm{R}}\times N_t^{\mathrm{S}}}$, $\boldsymbol{H}^{SD}\in\mathbb{C}^{N_r^{\mathrm{D}}\times N_t^{\mathrm{S}}}$, and $\boldsymbol{H}^{RD}\in\mathbb{C}^{N_r^{\mathrm{D}}\times N_t^{\mathrm{R}}}$, respectively. Each element of the above matrices is modelled as an independent and identically distributed rv with $\mathscr{C}\mathscr{N}(0,\sigma_h^2)$ and the channel obeys the Rayleigh flat fading model, where σ_h^2 is equal to σ_{SR}^2, σ_{SD}^2 and σ_{RD}^2 for the corresponding three channel matrices. To take into account the path loss, the variances are defined as $\sigma_{SR}^2 \triangleq d_{SR}^{-\alpha}$, $\sigma_{SD}^2 \triangleq d_{SD}^{-\alpha}$ and $\sigma_{RD}^2 \triangleq d_{RD}^{-\alpha}$ where d_{SR}, d_{SD} and d_{RD} are the distances between *S*–*R*, *S*–*D* and *R*–*D*, respectively and α is the path loss exponent [6]. Signal-to-noise ratio (SNR) parameter is defined as received SNR at *D*.

An SM symbol is given as $\boldsymbol{x} = [\underbrace{0\ \ 0\ \ \cdots\ \ 0}_{l-1}\ x_q\ \underbrace{0\ \ \cdots\ \ 0}_{N_t^{\mathrm{S}}-l}]^{\mathrm{T}}$, where l is the index of the activated transmit antenna, x_q is the *M*-ary phase SK (*M*-PSK)/quadrature amplitude modulation (QAM) constellation symbol and it is assumed that $E\{\boldsymbol{x}^{\mathrm{H}}\boldsymbol{x}\} = 1$. In the first time slot, *S* transmits an SM symbol to *R* and *D* as

$$\boldsymbol{y}^{SR} = \boldsymbol{H}^{SR}\boldsymbol{x} + \boldsymbol{n}^{SR} \tag{1}$$

$$\boldsymbol{y}^{SD} = \boldsymbol{H}^{SD}\boldsymbol{x} + \boldsymbol{n}^{SD} \tag{2}$$

respectively, where $\boldsymbol{n}^{SR(SD)}\in\mathbb{C}^{N_r^{\mathrm{R}}(N_r^{\mathrm{D}})\times 1}$ is the additive white Gaussian noise (AWGN) samples vector whose entries are modelled as $\mathscr{C}\mathscr{N}(0,N_0)$ with noise spectral density $N_0/2$ per dimension.

2.1 DF cooperative SM

In the second time slot, the detector at *R*, which has the ideal channel state information, detects the SM symbol applying the ML decision rule as

$$(\tilde{l},\tilde{x}_q) = \arg\min_{l,x_q} \|\boldsymbol{y}^{SR} - \boldsymbol{H}^{SR}\boldsymbol{x}\|^2 \tag{3}$$

and re-encodes into a new SM symbol by considering $\tilde{l}$ and $\tilde{x}_q$ as $\tilde{\boldsymbol{x}} = [\underbrace{0\ \ 0\ \ \cdots\ \ 0}_{\tilde{l}-1}\ \tilde{x}_q\ \underbrace{0\ \ \cdots\ \ 0}_{N_t^{\mathrm{R}}-\tilde{l}}]^{\mathrm{T}}$ and sends it to *D*, which is received as

$$\boldsymbol{y}^{RD} = \boldsymbol{H}^{RD}\tilde{\boldsymbol{x}} + \boldsymbol{n}^{RD} \tag{4}$$

where $\boldsymbol{n}^{RD}\in\mathbb{C}^{N_r^{\mathrm{D}}\times 1}$ is the AWGN samples vector whose entries are distributed with $\mathscr{C}\mathscr{N}(0,N_0)$. From (2) and (4), the ML detection rule at *D* is given by

$$(\hat{l},\hat{x}_q) = \arg\min_{l,x_q}\left(\|\boldsymbol{y}^{SD} - \boldsymbol{H}^{SD}\boldsymbol{x}\|^2 + \|\boldsymbol{y}^{RD} - \boldsymbol{H}^{RD}\boldsymbol{x}\|^2\right). \tag{5}$$

2.2 AF cooperative SM

In MIMO-AF system, R amplifies the received signal at each receive antenna and sends to D from the same antenna as seen from Fig. 2 ($N_t^R = N_r^R = N^R$). The received signal vector at D becomes

$$\begin{aligned} \boldsymbol{y}^{RD} &= G\boldsymbol{H}^{RD}\boldsymbol{y}^{SR} + \boldsymbol{n}^{RD} \\ &= G\boldsymbol{H}^{RD}\boldsymbol{H}^{SR}\boldsymbol{x} + \boldsymbol{n}_{\text{MIMO}} \end{aligned} \tag{6}$$

where $G = \sqrt{1/(N_t^R(\sigma_{SR}^2 + N_0))}$ (in G, $\sqrt{1/N_t^R}$ is the scaling factor for the normalisation of the transmitted energy at R), $\boldsymbol{n}_{\text{MIMO}}$ is the coloured Gaussian noise vector and can be expressed as

$$\boldsymbol{n}_{\text{MIMO}} = G\boldsymbol{H}^{RD}\boldsymbol{n}^{SR} + \boldsymbol{n}^{RD} \tag{7}$$

with the conditional covariance matrix

$$\begin{aligned} \boldsymbol{C} &= E\left\{\boldsymbol{n}_{\text{MIMO}}\boldsymbol{n}_{\text{MIMO}}^{\text{H}} \mid \boldsymbol{H}^{RD}\right\} \\ &= G^2\boldsymbol{H}^{RD}\left(\boldsymbol{H}^{RD}\right)^{\text{H}}N_0 + N_0\boldsymbol{I}_{N_r^{\text{D}}}. \end{aligned} \tag{8}$$

ML detection rule at D is given for the MIMO-AF system as [19] (see (9))

3 ABEP analysis for DF relaying

The ABEP of the cooperative SM system can be evaluated using the average PEP (APEP) which is computed next.

APEP at D for the MIMO-DF cooperative SM system is upper bounded as (see (10)) where $P_{\text{R}}(\boldsymbol{x} \to \tilde{\boldsymbol{x}})$ is the APEP at R when $\boldsymbol{x}$ is transmitted and it is erroneously detected as $\tilde{\boldsymbol{x}}$, $P_{\text{R}}^{\text{c}}(\boldsymbol{x})$ is the probability of correct decision at R, $P_{\text{D}}(\boldsymbol{x} \to \hat{\boldsymbol{x}} \mid R{:}\boldsymbol{x})$ is the APEP at D when R detects the SM symbol correctly and $P_{\text{D}}(\boldsymbol{x} \to \hat{\boldsymbol{x}} \mid R{:}\tilde{\boldsymbol{x}})$ is the APEP at D when R makes a decoding error.

$P_{\text{D}}(\boldsymbol{x} \to \hat{\boldsymbol{x}} \mid R{:}\tilde{\boldsymbol{x}})$ can be calculated for all possible $\tilde{\boldsymbol{x}}$ as (see (11))

(see (12))

which simplifies to (see (13)) .

When the transmitted SM symbol $\boldsymbol{x}$ is erroneously detected as

$$\hat{\boldsymbol{x}} = [\underbrace{0 \quad 0 \quad \dots \quad 0}_{\hat{l}-1}\ \hat{x}_q\ \underbrace{0 \quad \dots \quad 0}_{N_t-\hat{l}}]^{\text{T}}$$

at both R and D, i.e. for the case of $\tilde{\boldsymbol{x}} = \hat{\boldsymbol{x}}$, (13) can be written as (see (14)) .

Since the Q-function strictly decreases, (14) is greater than (13). Moreover, at high SNR values ($N_0 \to 0$), (14) can be approximated as [20] (see (15)) .

Since the right- and left-hand sides of the inequality in (15) follow the same distribution, this probability equals 0.5. This implies that ABEP of MIMO-DF cooperative SM system is dominated by the case of $\tilde{\boldsymbol{x}} = \hat{\boldsymbol{x}}$. Therefore, (10) can be approximated as (see (16)) .

$P_{\text{R}}(\boldsymbol{x} \to \hat{\boldsymbol{x}})$ is the APEP of the conventional SM and can be formulated as

$$\begin{aligned} P_{\text{R}}(\boldsymbol{x} \to \hat{\boldsymbol{x}}) &= E\left\{ \Pr\left\{\boldsymbol{x} \to \hat{\boldsymbol{x}} \mid \boldsymbol{H}^{SR}\right\}\right\} \\ &= E\left\{Q\left(\sqrt{\frac{\| \boldsymbol{H}^{SR}(\boldsymbol{x} - \hat{\boldsymbol{x}}) \|^2}{2N_0}}\right)\right\}. \end{aligned} \tag{17}$$

$P_{\text{R}}^{\text{c}}(\boldsymbol{x})$ is also dominated by the case of $\tilde{\boldsymbol{x}} = \hat{\boldsymbol{x}}$ and can be approximated as $P_{\text{R}}^{\text{c}}(\boldsymbol{x}) \simeq \left(1 - P_{\text{R}}(\boldsymbol{x} \to \hat{\boldsymbol{x}})\right)$.

Since $P_{\text{D}}(\boldsymbol{x} \to \hat{\boldsymbol{x}} \mid R{:}\boldsymbol{x})$ is the APEP at D when R detects the SM symbol correctly, the antenna index and the data symbol are detected properly, i.e. $\tilde{l} = l$ and $\tilde{x}_q = x_q$. For this case, by substituting $\tilde{\boldsymbol{x}} = \boldsymbol{x}$ in (13), $P_{\text{D}}(\boldsymbol{x} \to \hat{\boldsymbol{x}} \mid R{:}\boldsymbol{x})$ simplifies to

$$P_{\text{D}}(\boldsymbol{x} \to \hat{\boldsymbol{x}} \mid R{:}\boldsymbol{x}) = E\left\{Q\left(\sqrt{\frac{\| \boldsymbol{H}^{SD}(\boldsymbol{x} - \hat{\boldsymbol{x}}) \|^2 + \| \boldsymbol{H}^{RD}(\boldsymbol{x} - \hat{\boldsymbol{x}}) \|^2}{2N_0}}\right)\right\}. \tag{18}$$

To obtain the APEP, the pdf's of the rv's in Q-function of (17) and (18) have to be computed. Let $\gamma^{SR} \triangleq (\rho/2)\| \boldsymbol{H}^{SR}(\boldsymbol{x} - \hat{\boldsymbol{x}}) \|^2$ with

$$(\hat{l}, \hat{x}_q) = \arg\min_{l,q}\left(\| \boldsymbol{y}^{SD} - \boldsymbol{H}^{SD}\boldsymbol{x} \|^2/N_0 + \| \boldsymbol{C}^{-1/2}\left(\boldsymbol{y}^{RD} - G\boldsymbol{H}^{RD}\boldsymbol{H}^{SR}\boldsymbol{x}\right) \|^2\right). \tag{9}$$

$$P_{\text{D}}^{DF}(\boldsymbol{x} \to \hat{\boldsymbol{x}}) \le P_{\text{R}}^{\text{c}}(\boldsymbol{x})P_{\text{D}}(\boldsymbol{x} \to \hat{\boldsymbol{x}} \mid R{:}\boldsymbol{x}) + \sum_{\substack{\tilde{\boldsymbol{x}} \\ \tilde{\boldsymbol{x}} \ne \boldsymbol{x}}} P_{\text{R}}(\boldsymbol{x} \to \tilde{\boldsymbol{x}})P_{\text{D}}(\boldsymbol{x} \to \hat{\boldsymbol{x}} \mid R{:}\tilde{\boldsymbol{x}}) \tag{10}$$

$$\begin{aligned} P_{\text{D}}(\boldsymbol{x} \to \hat{\boldsymbol{x}} \mid R{:}\tilde{\boldsymbol{x}}) = E\Big\{ \Pr\Big\{&\| \boldsymbol{y}^{SD} - \boldsymbol{H}^{SD}\boldsymbol{x} \|^2 + \| \boldsymbol{y}^{RD} - \boldsymbol{H}^{RD}\boldsymbol{x} \|^2 \\ &\ge \| \boldsymbol{y}^{SD} - \boldsymbol{H}^{SD}\hat{\boldsymbol{x}} \|^2 + \| \boldsymbol{y}^{RD} - \boldsymbol{H}^{RD}\hat{\boldsymbol{x}} \|^2 \mid \boldsymbol{H}^{SD}, \boldsymbol{H}^{RD}\Big\}\Big\} \end{aligned} \tag{11}$$

$$\begin{aligned} = E\Big\{ \Pr\Big\{&\| \left(\boldsymbol{H}^{SD}\boldsymbol{x} + \boldsymbol{n}^{SD}\right) - \boldsymbol{H}^{SD}\boldsymbol{x} \|^2 + \| \left(\boldsymbol{H}^{RD}\tilde{\boldsymbol{x}} + \boldsymbol{n}^{RD}\right) - \boldsymbol{H}^{RD}\boldsymbol{x} \|^2 \\ &\ge \| \left(\boldsymbol{H}^{SD}\boldsymbol{x} + \boldsymbol{n}^{SD}\right) - \boldsymbol{H}^{SD}\hat{\boldsymbol{x}} \|^2 \\ &\quad + \| \left(\boldsymbol{H}^{RD}\tilde{\boldsymbol{x}} + \boldsymbol{n}^{RD}\right) - \boldsymbol{H}^{RD}\hat{\boldsymbol{x}} \|^2 \mid \boldsymbol{H}^{SD}, \boldsymbol{H}^{RD}\Big\}\Big\} \end{aligned} \tag{12}$$

$$P_{\text{D}}(\boldsymbol{x} \to \hat{\boldsymbol{x}} \mid R{:}\tilde{\boldsymbol{x}}) = E\left\{Q\left(\frac{\| \boldsymbol{H}^{SD}(\boldsymbol{x} - \hat{\boldsymbol{x}}) \|^2 + \| \boldsymbol{H}^{RD}(\tilde{\boldsymbol{x}} - \hat{\boldsymbol{x}}) \|^2 - \| \boldsymbol{H}^{RD}(\tilde{\boldsymbol{x}} - \boldsymbol{x}) \|^2}{\sqrt{2N_0\left(\| \boldsymbol{H}^{SD}(\boldsymbol{x} - \hat{\boldsymbol{x}}) \|^2 + \| \boldsymbol{H}^{RD}(\tilde{\boldsymbol{x}} - \hat{\boldsymbol{x}}) \|^2 + \| \boldsymbol{H}^{RD}(\tilde{\boldsymbol{x}} - \boldsymbol{x}) \|^2\right)}}\right)\right\}. \tag{13}$$

$$P_{\text{D}}(\boldsymbol{x} \to \hat{\boldsymbol{x}} \mid R{:}\hat{\boldsymbol{x}}) = E\left\{Q\left(\frac{\| \boldsymbol{H}^{SD}(\boldsymbol{x} - \hat{\boldsymbol{x}}) \|^2 - \| \boldsymbol{H}^{RD}(\hat{\boldsymbol{x}} - \boldsymbol{x}) \|^2}{\sqrt{2N_0\left(\| \boldsymbol{H}^{SD}(\boldsymbol{x} - \hat{\boldsymbol{x}}) \|^2 + \| \boldsymbol{H}^{RD}(\hat{\boldsymbol{x}} - \boldsymbol{x}) \|^2\right)}}\right)\right\}. \tag{14}$$

the pdf $f_{\gamma^{SR}}(\gamma)$, $\gamma^{SR} \geq 0$ where $\rho = (1/N_0)$. The APEP at R can be calculated as

$$P_{\rm R}(\boldsymbol{x} \rightarrow \hat{\boldsymbol{x}}) = \int_0^\infty Q\left(\sqrt{\gamma^{SR}}\right) f_{\gamma^{SR}}(\gamma)\,\mathrm{d}\gamma \tag{19}$$

which can be computed with Craig's formula [21]. Using the alternative form of the Q-function in (19) yields

$$P_{\rm R}(\boldsymbol{x} \rightarrow \hat{\boldsymbol{x}}) = \frac{1}{\pi}\int_0^{\pi/2} M_{\gamma^{SR}}\left(-\frac{1}{2\sin^2\theta}\right)\mathrm{d}\theta \tag{20}$$

where $M_{\gamma^{SR}}(s)$ is the MGF of γ^{SR}. For the Rayleigh flat fading channel model, γ^{SR} follows the gamma distribution (in this special case, in fact, it follows Erlang distribution) with $\mathrm{Gamma}\left(N_r^{\rm R}, (\rho\lambda_x\sigma_{SR}^2/2)\right)$, where λ_x is the single eigenvalue of $(\boldsymbol{x} - \hat{\boldsymbol{x}})(\boldsymbol{x} - \hat{\boldsymbol{x}})^{\rm H}$ and is equal to

$$\lambda_x = \begin{cases} |x_q - \hat{x}_q|^2 & \text{if} \quad l = \hat{l} \\ |x_q|^2 + |\hat{x}_q|^2 & \text{if} \quad l \neq \hat{l}\,. \end{cases} \tag{21}$$

The MGF of γ^{SR} is obtained as [21]

$$M_{\gamma^{SR}}(s) = \left(1 - \frac{\rho\lambda_x\sigma_{SR}^2}{2}s\right)^{-N_r^{\rm R}}. \tag{22}$$

(20) can be computed using (5A.4a) of [21] as

$$P_{\rm R}(\boldsymbol{x} \rightarrow \hat{\boldsymbol{x}}) = \frac{1}{2}\left[1 - \mu\sum_{j=0}^{N_r^{\rm R}-1}\binom{2j}{j}\left(\frac{1-\mu^2}{4}\right)^j\right] \tag{23}$$

where $\mu = \sqrt{(\rho\lambda_x\sigma_{SR}^2/4)/((\rho\lambda_x\sigma_{SR}^2/4) + 1)}$. The same procedures can also be followed for the calculation of $P_{\rm D}(\boldsymbol{x} \rightarrow \hat{\boldsymbol{x}} \mid R{:}\boldsymbol{x})$.

Let us consider

$$\begin{aligned} \gamma^{DF} &= \frac{\rho}{2}\left(\|\,\boldsymbol{H}^{SD}(\boldsymbol{x} - \hat{\boldsymbol{x}})\,\|^2 + \|\,\boldsymbol{H}^{RD}(\boldsymbol{x} - \hat{\boldsymbol{x}})\,\|^2\right) \\ &= \gamma^{SD} + \gamma^{RD}. \end{aligned} \tag{24}$$

(24) is the sum of two Gamma rv's with different scale parameters. The MGF of (24) can be written as

$$M_{\gamma^{DF}}(s) = \left(1 - \frac{\rho\lambda_x\sigma_{SD}^2}{2}s\right)^{-N_r^{\rm D}}\left(1 - \frac{\rho\lambda_x\sigma_{RD}^2}{2}s\right)^{-N_r^{\rm D}}. \tag{25}$$

Therefore, $P_{\rm D}(\boldsymbol{x} \rightarrow \hat{\boldsymbol{x}} \mid R{:}\boldsymbol{x})$ can be written as

$$P_{\rm D}(\boldsymbol{x} \rightarrow \hat{\boldsymbol{x}} \mid R{:}\boldsymbol{x}) = \frac{1}{\pi}\int_0^{\pi/2} M_{\gamma^{DF}}\left(-\frac{1}{2\sin^2\theta}\right)\mathrm{d}\theta \tag{26}$$

which can be calculated with the help of Appendix 5A.58 of [21].

On the other hand, the pdf of γ^{DF} follows the distribution of the sum of two gamma rv's as $\mathrm{Gamma}\left(2N_r^{\rm D}, (\rho\lambda_x\sigma^2/2)\right)$ when $\sigma_{SD}^2 = \sigma_{RD}^2 = \sigma^2$. Therefore, its MGF is given as

$$M_{\gamma^{DF}}(s) = \left(1 - \frac{\rho\lambda_x\sigma^2}{2}s\right)^{-2N_r^{\rm D}}. \tag{27}$$

As a result, $P_{\rm D}(\boldsymbol{x} \rightarrow \hat{\boldsymbol{x}} \mid R{:}\boldsymbol{x})$ is obtained as

$$P_{\rm D}(\boldsymbol{x} \rightarrow \hat{\boldsymbol{x}} \mid R{:}\boldsymbol{x}) = \frac{1}{2}\left[1 - \mu\sum_{j=0}^{2N_r^{\rm D}-1}\binom{2j}{j}\left(\frac{1-\mu^2}{4}\right)^j\right] \tag{28}$$

where μ is as defined in (23).

After computing the APEP, the ABEP can be averaged as [22]

$$P_b^{DF} \simeq \frac{1}{N_t M \log_2(N_t M)}\sum_{\boldsymbol{x}}\sum_{\substack{\hat{\boldsymbol{x}} \\ \hat{\boldsymbol{x}} \neq \boldsymbol{x}}} n(\boldsymbol{x} \rightarrow \hat{\boldsymbol{x}}) P_{\rm D}^{DF}(\boldsymbol{x} \rightarrow \hat{\boldsymbol{x}}) \tag{29}$$

where $n(\boldsymbol{x} \rightarrow \hat{\boldsymbol{x}})$ is the number of BEs between the SM symbols $\boldsymbol{x}$ and $\hat{\boldsymbol{x}}$.

An upper limit can be obtained when $\theta = \pi/2$ is used in the integrand function of (20) and (26). Therefore, $P_{\rm R}(\boldsymbol{x} \rightarrow \hat{\boldsymbol{x}})$ and $P_{\rm D}(\boldsymbol{x} \rightarrow \hat{\boldsymbol{x}} \mid R{:}\boldsymbol{x})$ are upper bounded as

$$P_{\rm R}(\boldsymbol{x} \rightarrow \hat{\boldsymbol{x}}) \leq \left(1 + \frac{\rho\lambda_x\sigma_{SR}^2}{4}\right)^{-N_r^{\rm R}} \tag{30}$$

$$P_{\rm D}(\boldsymbol{x} \rightarrow \hat{\boldsymbol{x}} \mid R{:}\boldsymbol{x}) \leq \left(1 + \frac{\rho\lambda_x\sigma_{SD}^2}{4}\right)^{-N_r^{\rm D}}\left(1 + \frac{\rho\lambda_x\sigma_{RD}^2}{4}\right)^{-N_r^{\rm D}}. \tag{31}$$

We can easily see from (16), (30) and (31) that when SNR $\rightarrow \infty$, i.e. $(\rho\lambda_x\sigma_{SR,RD,SD}^2)/4 \rightarrow \infty$, the diversity order can be achieved as $\min\left\{N_r^{\rm R}, 2N_r^{\rm D}\right\}$. Note that, when $\sigma_{SR}^2 = d_{SR}^{-\alpha} \gg \sigma_{SD}^2, \sigma_{RD}^2$, i.e. R close to S, R detects the signal correctly with a high probability and (31) dominates compared with (30). Therefore, the diversity order will be $2N_r^{\rm D}$.

4 ABEP analysis for AF relaying

The APEP at D for the SM MIMO-AF system can be calculated as (see (32)) Following the same steps as in (12) and after simplifications, (32) can be rewritten as:

$$P_{\rm D}^{AF}(\boldsymbol{x} \rightarrow \hat{\boldsymbol{x}}) = E\left\{Q\left(\sqrt{\gamma^{SD} + \gamma^{SRD}}\right)\right\} \tag{33}$$

where γ^{SD} is same as in (24) and for source-relay-destination (SRD), γ^{SRD} is given as

$$\gamma^{SRD} = \frac{G^2\|\,\boldsymbol{C}^{-1/2}\boldsymbol{H}^{RD}\boldsymbol{H}^{SR}(\boldsymbol{x} - \hat{\boldsymbol{x}})\,\|^2}{2}. \tag{34}$$

$$P_{\rm D}(\boldsymbol{x} \rightarrow \hat{\boldsymbol{x}} \mid R{:}\hat{\boldsymbol{x}}) \simeq \Pr\left(\|\,\boldsymbol{H}^{SD}(\boldsymbol{x} - \hat{\boldsymbol{x}})\,\|^2 < \|\,\boldsymbol{H}^{RD}(\boldsymbol{x} - \hat{\boldsymbol{x}})\,\|^2 \mid \boldsymbol{H}^{SD}, \boldsymbol{H}^{RD}\right). \tag{15}$$

$$P_{\rm D}^{DF}(\boldsymbol{x} \rightarrow \hat{\boldsymbol{x}}) \simeq P_{\rm R}^{\rm c}(\boldsymbol{x})P_{\rm D}(\boldsymbol{x} \rightarrow \hat{\boldsymbol{x}} \mid R{:}\boldsymbol{x}) + P_{\rm R}(\boldsymbol{x} \rightarrow \hat{\boldsymbol{x}})P_{\rm D}(\boldsymbol{x} \rightarrow \hat{\boldsymbol{x}} \mid R{:}\hat{\boldsymbol{x}}). \tag{16}$$

$$\begin{aligned} P_{\rm D}^{AF}(\boldsymbol{x} \rightarrow \hat{\boldsymbol{x}}) = E\Big\{ &\Pr\Big\{\|\,\boldsymbol{y}^{SD} - \boldsymbol{H}^{SD}\boldsymbol{x}\,\|^2/N_0 + \|\,\boldsymbol{C}^{-1/2}\left(\boldsymbol{y}^{RD} - G\boldsymbol{H}^{RD}\boldsymbol{H}^{SR}\boldsymbol{x}\right)\|^2 \\ &\geq \|\,\boldsymbol{y}^{SD} - \boldsymbol{H}^{SD}\hat{\boldsymbol{x}}\,\|^2/N_0 + \|\,\boldsymbol{C}^{-1/2}\left(\boldsymbol{y}^{RD} - G\boldsymbol{H}^{RD}\boldsymbol{H}^{SR}\hat{\boldsymbol{x}}\right)\|^2 \mid \boldsymbol{H}^{SD}, \boldsymbol{H}^{SR}, \boldsymbol{H}^{RD}\Big\}\Big\}. \end{aligned} \tag{32}$$

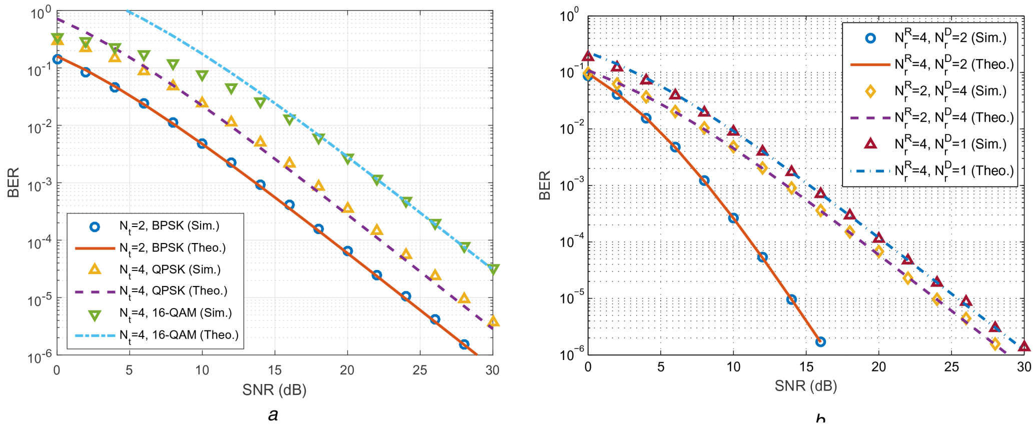

Fig. 3 *BER performance of cooperative SM system with DF relaying*
(a) For different numbers of transmit antennas and modulation orders, $N_t^S = N_t^R = N_t$ and $N_r^R = N_r^D = 2$, ***(b)*** For different numbers of receive antennas at R and D, $N_t^S = N_t^R = N_t = 2$, $M = 2$ [binary PSK(BPSK)]

The MGF of γ^{SD} can be calculated as in (22). On the other hand, the MGF of γ^{SRD} is given as (see the Appendix)

$$M_{\gamma^{SRD}}(s) = \frac{\det(\boldsymbol{\Phi})}{\prod_{n=1}^{r_{\min}} \Gamma(r_{\max} - n + 1)\Gamma(r_{\min} - n + 1)} \tag{35}$$

where $r_{\min} = \min\{N^R, N_r^D\}$, $r_{\max} = \max\{N^R, N_r^D\}$ and $\boldsymbol{\Phi}$ is an $r_{\min} \times r_{\min}$ Hankel matrix whose (n,m)th entry is obtained as

$$\Phi_{n,m} = z^{-\eta}\Gamma(\eta)U\left(\eta, \eta, \frac{1}{z}\right) + G^2 z^{-\eta-1}\Gamma(\eta+1)U\left(\eta+1, \eta+1, \frac{1}{z}\right) \tag{36}$$

where $z = G^2(1 - (\rho\lambda_x s\sigma_{SR}^2/2))$, $\eta = r_{\max} - r_{\min} + n + m - 1$ and $U(\cdot,\cdot,\cdot)$ is the confluent hypergeometric function of the second kind.

Using Craig's formula again, (33) is expressed as

$$P_D^{AF}(\boldsymbol{x} \to \hat{\boldsymbol{x}}) = \frac{1}{\pi}\int_0^{\pi/2} M_{\gamma^{SD}}\left(-\frac{1}{2\sin^2\theta}\right)M_{\gamma^{SRD}}\left(-\frac{1}{2\sin^2\theta}\right)\mathrm{d}\theta \tag{37}$$

where numerical integration is needed. When the numerical integration is not used, (37) can be simplified and upper bounded as

$$P_D^{AF}(\boldsymbol{x} \to \hat{\boldsymbol{x}}) < \frac{1}{\pi}M_{\gamma^{SD}}\left(-\frac{1}{2}\right)M_{\gamma^{SRD}}\left(-\frac{1}{2}\right) \tag{38}$$

ABEP can be obtained using the union bound as [22]

$$P_b^{AF} \le \frac{1}{N_t M \log_2(N_t M)}\sum_{\boldsymbol{x}}\sum_{\substack{\hat{\boldsymbol{x}} \\ \hat{\boldsymbol{x}} \ne \boldsymbol{x}}} n(\boldsymbol{x} \to \hat{\boldsymbol{x}})P_D^{AF}(\boldsymbol{x} \to \hat{\boldsymbol{x}}). \tag{39}$$

On the other hand, when SNR $\to \infty$, i.e. $\lambda_x\sigma_{SD(SR)}^2/N_0 \to \infty$, (38) is approximated to

$$P_D^{AF}(\boldsymbol{x} \to \hat{\boldsymbol{x}}) \simeq \frac{1}{\pi}\left(1 + \frac{\rho\lambda_x\sigma_{SD}^2}{4}\right)^{-N_r^D}\left(G^2\left(1 + \frac{\rho\lambda_x\sigma_{SR}^2}{4}\right)\right)^{-r_{\min}} \tag{40}$$

where we use $U(a,b,z) \simeq z^{1-b}$ for small z [23]. Finally, the diversity order of the MIMO-AF system can be observed from (40) as $N_r^D + \min\{N^R, N_r^D\}$.

5 Performance evaluation

In this section, analytical and computer simulation results for the BEP of cooperative SM systems are presented. Moreover, BER performance comparisons of the cooperative SM (both AF and DF) and classical cooperative systems are performed. In these comparisons, classical cooperative systems are selected as in [6], where the considered modulation is classical M-PSK or QAM. On the other hand, modulation order is chosen to provide the same spectral efficiency as in the cooperative SM systems. Since, only a single transmit antenna is active in the SM systems, a single antenna is employed for classical M-PSK/QAM systems ($N_t^S = 1$). At receiver, maximum ratio combining is considered for classical cooperative systems. Monte Carlo simulations are performed for at least 10^6 channel uses as a function of the received SNR at D and compared with the analytical results. The path loss exponent is chosen as $\alpha = 3$.

5.1 Results for DF relaying

To obtain the same spectral efficiency, the number of transmit antennas and modulation orders are taken identical for S–R and R–D links, i.e. $N_t^S = N_t^R = N_t$ and $M^S = M^R = M$ for MIMO-DF relaying.

BER performance of the cooperative SM system with DF relaying is given in Fig. 3*a*. The number of receive antennas for R and D are considered as the same, i.e. $N_r^R = N_r^D = 2$. The computer simulations are evaluated for different spectral efficiencies by considering different numbers of transmit antennas and modulation orders. As seen from Fig. 3*a*, theoretical curves closely match with computer simulation results at high SNR due to the use of BER union bound.

In Fig. 3*b*, the effect of number of receive antennas on the BER performance is investigated. Computer simulation results are depicted for $N_t^S = N_t^R = 2$, $M = 2$ (BPSK) and different numbers of receive antennas at R and D. As seen from Fig. 3*b*, since the lower modulation orders and number of transmit/receive antennas are chosen, the analytical curves and computer simulation results are in close match also at lower SNR values. On the other hand, the slope of the curves, i.e. the diversity order, depends on the number of receive antennas at R and D, i.e. $\min\{N_r^R, 2N_r^D\}$. In Figs. 3*a* and *b*, unit distances are considered between all nodes, i.e. $d_{SD} = d_{SR} = d_{RD} = 1$.

In Fig. 4, the effect of different distances between nodes on the BER performance is evaluated both analytically and theoretically. The SM parameters are chosen as $N_t^S = 2$, $M = 2$ (BPSK) and the number of receive antennas at R and D is $N_r^R = N_r^D = 2$. A unit distance is assumed between S–D and R–D ($d_{SD} = d_{RD} = 1$), and the following three different cases are considered for the distances between S and R: $d_{SR} = 0.3$, $d_{SR} = 0.7$ and $d_{SR} = 1$. It can be seen from Fig. 4 that the BER performance of DF relaying, more specifically the diversity order, improves when R gets closer to S. For this case, σ_{SR}^2 becomes larger than σ^2 and when the SNR goes to infinity, (31) dominates the diversity order that converges to $2N_r^D$.

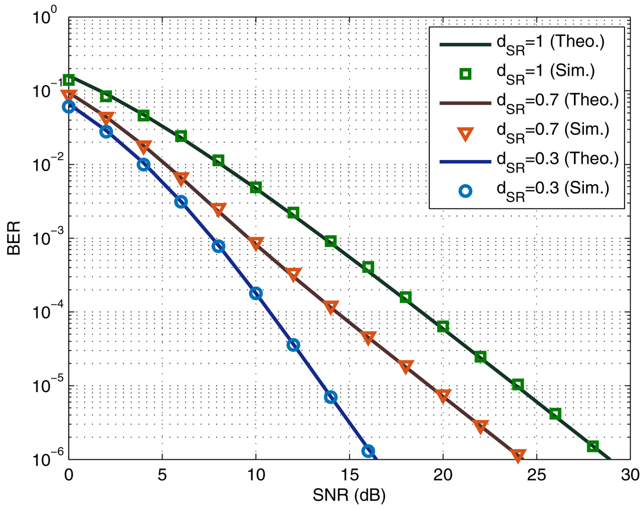

Fig. 4 *BER performance of cooperative SM system with DF relaying for different relay locations ($d_{SD} = d_{RD} = 1$)*

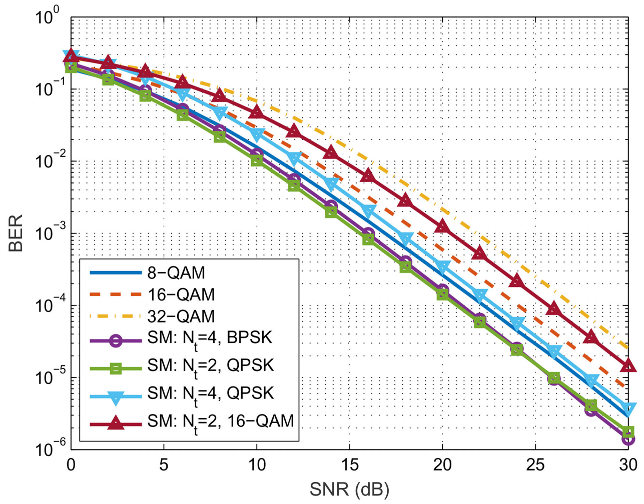

Fig. 5 *BER performance comparison of cooperative SM with classical cooperative M-ary modulation for DF relaying systems ($N_r^{\mathrm{R}} = N_r^{\mathrm{D}} = N_r = 2$)*

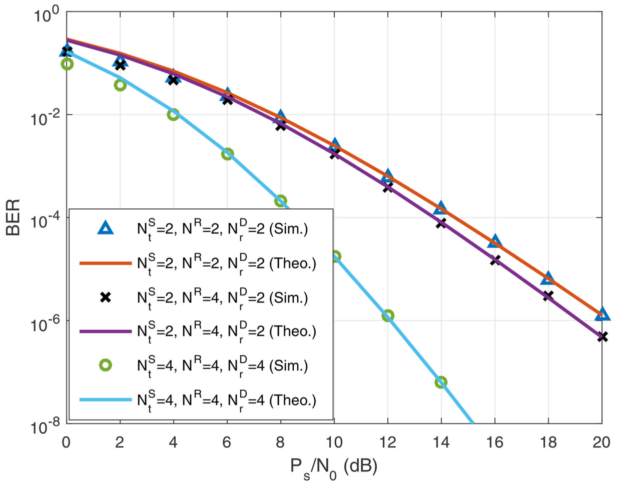

Fig. 6 *BER performance of SM MIMO-AF relaying with different configurations. $N_t^{\mathrm{R}} = N_r^{\mathrm{R}} = N^{\mathrm{R}}$ with quadrature PSK (QPSK)*

The BER performance comparison of cooperative SM and classical cooperative M-ary modulated systems for $R = 3$, 4 and 5 bits/s/Hz spectral efficiencies is given in Fig. 5, where $R = \log_2(N_t M)$ assuming two receive antennas at R and D. As seen from Fig. 5, cooperative SM system provides 2 dB SNR gain over

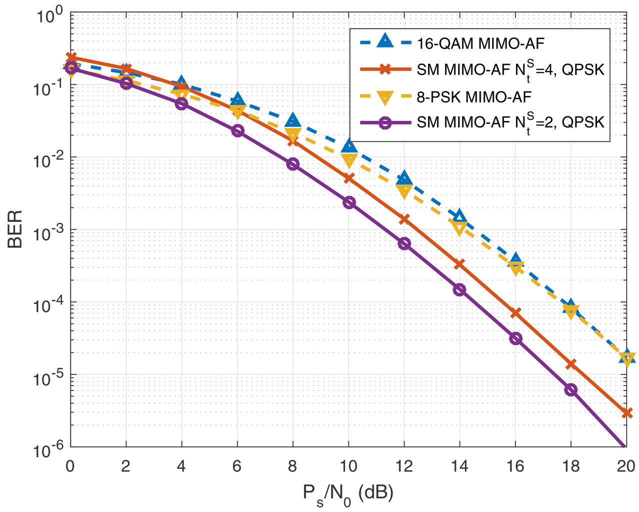

Fig. 7 *BER comparison of MIMO-AF cooperative SM system with classical M-PSK/QAM modulated cooperative system ($N_t^R = N_r^R = N_r^D = 2$)*

the corresponding classical APM modulated cooperative system when R and D have two receive antennas.

5.2 Results for AF relaying

Computer simulations are performed as a function of the power spent at S to noise ratio (P_S/N_0) for AF relaying. The power spent at R is taken equal to P_{S}, i.e. $P_{\mathrm{S}} = P_{\mathrm{R}}$. In all computer simulations, unit power is assumed at each nodes.

Theoretical and computer simulation results for AF relaying are given in Fig. 6, where three different SM configurations are considered: (i) $N_t^{\mathrm{S}} = 2$, $N_t^{\mathrm{R}} = N_r^{\mathrm{R}} = N^{\mathrm{R}} = 2$, $N_r^{\mathrm{D}} = 2$, (ii) $N_t^{\mathrm{S}} = 2$, $N^{\mathrm{R}} = 4$, $N_r^{\mathrm{D}} = 2$, and (iii) $N_t^{\mathrm{S}} = 4$, $N^{\mathrm{R}} = 4$, $N_r^{\mathrm{D}} = 4$. For all configurations QPSK is considered. As seen from Fig. 6, theoretical results exactly match with the computer simulation results at high SNR values.

In Fig. 7, the BER comparison of MIMO-AF cooperative SM system and classical M-PSK/QAM modulated cooperative system with ML decision at D is given for $R = 3$ and 4 bits/s/Hz spectral efficiencies. The classical modulated systems also use all of the available antennas at R, denoted by M-PSK/QAM MIMO-AF. Since only a single transmit antenna is active in the SM system, number of transmit antennas for classical M-PSK/QAM system is chosen as $N_t^{\mathrm{S}} = 1$. The number of transmit/receive antennas for R and D is $N_r^{\mathrm{R}} = N_r^{\mathrm{D}} = 2$ for both systems. As seen from Fig. 7, the cooperative SM scheme provides better error performance than classical cooperative systems for the same spectral efficiency. It can be observed that the SM system provides 3 and 4 dB SNR gains for $R = 3$ and 4 bits/s/Hz spectral efficiencies, respectively.

5.3 Comparison of MIMO-DF and MIMO-AF systems

The comparison results of MIMO-DF and MIMO-AF cooperative SM systems can be found in Figs. 8*a* and *b*. SM parameters are chosen as $N_t^{\mathrm{S}} = 2$, $M = 2$ (QPSK) for both figures. In Fig. 8*a*, the effect of different numbers of receive antennas at R and D is investigated. When the number of receive antennas at R is lower, the error propagation has influence on the BER of the DF system, so that MIMO-AF system has better error performance. Otherwise, MIMO-DF system outperforms MIMO-AF.

Since the location of R directly affects the BER performance of the DF system, its impact is examined in Fig. 8*b*. As can be seen from Fig. 8*b*, when the links S–R and R–D have $d_{SR} = d_{RD} = 0.5$, MIMO-AF system provides better error performance above the SNR value of 5 dB. When R gets closer to S, i.e. $d_{SR} = 0.4$, MIMO-DF system exhibits better BER performance than MIMO-AF up to the SNR value of 12 dB. This shows that error propagation effect is still significant at these distances.

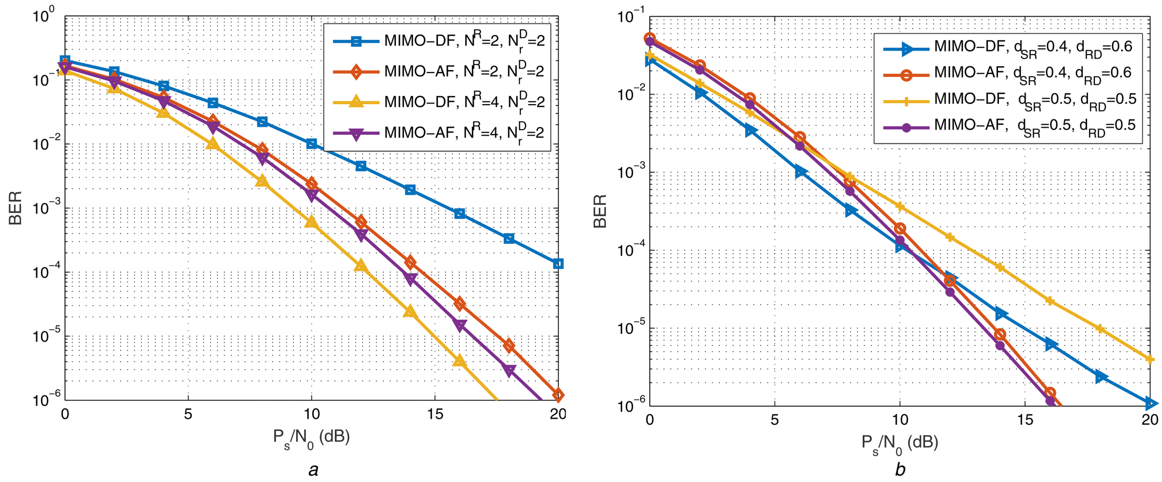

Fig. 8 *BER comparison of MIMO-AF and MIMO-DF cooperative SM systems*
(a) Under different number of receive antennas, $N_t^S = 2$, $M = 4$ (QPSK), ***(b)*** Under different R locations, $N_t^S = 2$, $M = 4$ (QPSK), $N^R = N_r^D = 2$, $d_{SD} = 1$

6 Conclusion

In this paper, we have investigated the ABEP performance of the cooperative SM scheme for AF and DF relaying. Most of the studies on cooperative SM systems in the literature consider only the SSK scheme with a single receive antenna at R and/or D. In this paper, we have derived analytical expressions for the ABEP of AF and DF multi-antenna cooperative communications systems that employ SM. We also have presented a diversity order analysis and have demonstrated the effect of relay location to DF relaying. Since the BER performance is derived analytically from the union bound, computer simulations and analytical results have shown that the derived expressions for the ABEP exactly match with the computer simulation results in high SNR region. We also have presented the comparison results of MIMO-DF and MIMO-AF relaying with classical M-PSK/QAM systems. For both relaying systems, SM technique provides error performance gain over conventional cooperative APM systems. Finally, the comparison results of MIMO-AF with MIMO-DF cooperative SM systems have been introduced. Investigation of real practical problems such as signalling design and synchronisation, channel estimation errors, resource management, interference etc. has been left as a future study.

7 Acknowledgments

This work was supported by The Scientific and Technological Research Council of Turkey (TÜBİTAK) under grant no. 114E607.

8 References

[1] Mesleh, R., Haas, H., Sinanovic, S., *et al.*: 'Spatial modulation', *IEEE Trans. Veh. Technol.*, 2008, **57**, (4), pp. 2228–2241
[2] Wolniansky, P., Foschini, G., Golden, G., *et al.*: 'V-BLAST: an architecture for realizing very high data rates over the rich-scattering wireless channel'. Proc. Int. Symp. Signals, Systems, Electronics (ISSSE'98), Pisa, Italy, September 1998, pp. 295–300
[3] Tarokh, V., Jafarkhani, H., Calderbank, A.: 'Space–time block codes from orthogonal designs', *IEEE Trans. Inf. Theory*, 1999, **16**, (8), pp. 1456–1467
[4] Jeganathan, J., Ghrayeb, A., Szczecinski, L., *et al.*: 'Space shift keying modulation for MIMO channels', *IEEE Trans. Wirel. Commun.*, 2009, **8**, (7), pp. 3692–3703
[5] Basar, E.: 'Index modulation techniques for 5G wireless networks', *IEEE Commun. Mag.*, 2016, **54**, (7), pp. 168–175
[6] Laneman, J.N., Tse, D.N.C., Wornell, G.W.: 'Cooperative diversity in wireless networks: efficient protocols and outage behavior', *IEEE Trans. Inf. Theory*, 2004, **50**, (12), pp. 3062–3080
[7] Serafimovski, N., Sinanovic, S., Di Renzo, M., *et al.*: 'Dual-hop spatial modulation (Dh-SM)'. Proc. IEEE Veh. Technol. Conf., Spring, Yokohoma, Japan, 2011
[8] Mesleh, R., Ikki, S.S., Alwakeel, M.: 'Performance analysis of space shift keying with AF relaying', *IEEE Commun. Lett.*, 2011, **15**, (12), pp. 1350–1352
[9] Mesleh, R., Ikki, S.S., Aggoune, E.H.M., *et al.*: 'Performance analysis of space shift keying (SSK) modulation with multiple cooperative relays', *EURASIP J. Adv. Signal Process.*, 2012, **201**, pp. 1–10
[10] Mesleh, R., Ikki, S.S.: 'Space shift keying with amplify-and-forward MIMO relaying', *Trans. Emerging Telecommun. Technol.*, 2015, **26**, (4), pp. 520–531
[11] Mesleh, R., Ikki, S.S.: 'Performance analysis of spatial modulation with multiple decode and forward relays', *IEEE Wirel. Commun. Lett.*, 2013, **2**, (4), pp. 423–426
[12] Som, P., Chockalingam, A.: 'End-to-end BER analysis of space shift keying in decode-and-forward cooperative relaying'. Proc. IEEE Wireless Communications Networking Conf., Shanghai, China, 2014, pp. 3465–3470
[13] Basar, E., Aygölü, Ü., Panayırcı, E., *et al.*: 'Space–time block coded spatial modulation', *IEEE Trans. Commun.*, 2011, **59**, (3), pp. 823–832
[14] Varshney, N., Goel, A., Jagannatham, A.K.: 'Cooperative communication in spatially modulated MIMO systems'. Proc. IEEE Wireless Communications and Networking Conf. (WCNC), Doha, Qatar, 2016
[15] Altın, G., Aygölü, Ü, Basar, E., *et al.*: 'Outage probability analysis of cooperative spatial modulation systems'. Proc. 23rd Int. Conf. Telecommunications (ICT), Greece, 2016, pp. 327–332
[16] Xie, X., Zhao, Z., Peng, M., *et al.*: 'Spatial modulation in two-way network coded channels: performance and mapping optimization'. Proc. IEEE Int. Symp. Personal Indoor, Mobile Radio Communications, Sydney, Australia, 2012
[17] Wen, M., Cheng, X., Poor, H.V., *et al.*: 'Use of SSK modulation in two-way amplify-and-forward relaying', *IEEE Trans. Veh. Technol.*, 2014, **63**, (3), pp. 1498–1504
[18] Som, P., Chockalingam, A.: 'Performance analysis of space shift keying in decode-and-forward multi-hop MIMO networks', *IEEE Trans. Veh. Technol.*, 2015, **64**, (1), pp. 132–146
[19] Zhang, K., Xiong, C., Chen, B., *et al.*: 'A maximum likelihood combining algorithm for spatial multiplexing MIMO amplify-and-forward relaying systems', *IEEE Trans. Veh. Technol.*, 2015, **64**, (12), pp. 5767–5774
[20] Basar, E., Aygölü, Ü, Panayırcı, E., *et al.*: 'A reliable successive relaying protocol', *IEEE Trans. Commun.*, 2014, **62**, (5), pp. 1431–1443
[21] Simon, M.K., Alouini, M.S.: '*Digital communication over fading channels*' (Wiley, Hoboken, NJ, 2005, 2nd edn.)
[22] Proakis, J.G.: '*Digital communications*' (McGraw-Hill, New York, NY, 2000, 4th edn.)
[23] Abramowitz, M., Stegun, I.A.: '*Handbook of mathematical functions with formulas, graphs, and mathematical tables*' (U.S. Department Commerce, Washington, DC, 1970)
[24] Clerckx, B., Oestges, C.: '*MIMO wireless networks: channels, techniques and standards for multi-antenna, multi-user and multi-cell systems*' (Elsevier/Academic Press, UK, 2013, 2nd edn.)
[25] Chiani, M., Win, M.Z., Zanella, A.: 'On the capacity of spatially correlated MIMO Rayleigh-fading channels', *IEEE Trans. Inf. Theory*, 2003, **49**, (10), pp. 2363–2371
[26] Tulino, A.M., Verdú, S.: 'Random matrix theory and wireless communications', *Found. Trends Commun. Inf. Theory*, 2004, **1**, (1), pp. 1–163

9 Appendix. Derivation of (35)

To find $M_{\gamma^{SRD}}$, we extend γ_{SRD}, given in (34), as

$$\gamma_{SRD} = \frac{G^2}{2}\mathrm{tr}\left(\left(\boldsymbol{H}^{RD}\right)^{\mathrm{H}}\boldsymbol{C}^{-1}\boldsymbol{H}^{RD}\boldsymbol{H}^{SR}(\boldsymbol{x}-\hat{\boldsymbol{x}})(\boldsymbol{x}-\hat{\boldsymbol{x}})^{\mathrm{H}}\left(\boldsymbol{H}^{SR}\right)^{\mathrm{H}}\right). \quad (41)$$

Using the eigenvalue decomposition for the Hermitian matrix $(\boldsymbol{x}-\hat{\boldsymbol{x}})(\boldsymbol{x}-\hat{\boldsymbol{x}})^{\mathrm{H}}$, we have

$$(\boldsymbol{x}-\hat{\boldsymbol{x}})(\boldsymbol{x}-\hat{\boldsymbol{x}})^{\mathrm{H}} = \boldsymbol{V}\boldsymbol{\Lambda}\boldsymbol{V}^{\mathrm{H}}. \quad (42)$$

Since the rank of the matrix $(\boldsymbol{x}-\hat{\boldsymbol{x}})(\boldsymbol{x}-\hat{\boldsymbol{x}})^{\mathrm{H}}$ is equal to one, we have a single eigenvalue λ_x and the corresponding eigenvector $\boldsymbol{v}$, where λ_x is as in (21) with the indices defined in $\hat{\boldsymbol{x}}$. Since the elements of the channel matrices are Gaussian rv's, the elements of the $\boldsymbol{H}^{SR}\boldsymbol{v}$ vector are also Gaussian. Let us define the vector $\boldsymbol{d} \triangleq \boldsymbol{H}^{SR}\boldsymbol{v}$, hence we obtain

$$\gamma_{SRD} = \frac{G^2\lambda_x}{2}\left(\boldsymbol{d}^{\mathrm{H}}\left(\boldsymbol{H}^{RD}\right)^{\mathrm{H}}\boldsymbol{C}^{-1}\boldsymbol{H}^{RD}\boldsymbol{d}\right). \tag{43}$$

The MGF of γ^{SRD} is given as

$$\begin{aligned} M_{\gamma^{SRD}}(s) &= E\left\{\mathrm{e}^{s\gamma^{SRD}}\right\} \\ &= E_{\boldsymbol{H}^{RD},\boldsymbol{d}}\left\{\exp\left(\frac{G^2\lambda_x s}{2}\left(\boldsymbol{d}^{\mathrm{H}}\left(\boldsymbol{H}^{RD}\right)^{\mathrm{H}}\boldsymbol{C}^{-1}\boldsymbol{H}^{RD}\boldsymbol{d}\right)\right)\right\}. \end{aligned} \tag{44}$$

As mentioned earlier, $\boldsymbol{d}$ is a complex Gaussian vector with the covariance matrix $\boldsymbol{R}_d = \sigma_{SR}^2\boldsymbol{I}_{N^{\mathrm{R}}}$ where $N_r^{\mathrm{R}} = N_{\mathrm{t}}^{\mathrm{R}} = N^{\mathrm{R}}$. Therefore, the MGF of γ^{SRD} given $\boldsymbol{H}^{RD}$ can be obtained from [24, Theorem D.1]

$$M_{\gamma^{SRD}\mid\boldsymbol{H}^{RD}}(s) = \frac{1}{\det\left(\boldsymbol{I}_{N^{\mathrm{R}}} - ((G^2\lambda_x\sigma_{SR}^2 s)/2)\left(\boldsymbol{H}^{RD}\right)^{\mathrm{H}}\boldsymbol{C}^{-1}\boldsymbol{H}^{RD}\right)}. \tag{45}$$

It is difficult to integrate (45) with respect to $\boldsymbol{H}^{RD}$. On the other hand, the eigenvalue decomposition of the Hermitian matrix $\boldsymbol{H}^{RD}\left(\boldsymbol{H}^{RD}\right)^{\mathrm{H}}$ can be used, i.e. $\boldsymbol{H}^{RD} = \boldsymbol{V}\boldsymbol{\Lambda}\boldsymbol{V}^{\mathrm{H}}$, where $\boldsymbol{V} \in \mathbb{C}^{N^{\mathrm{R}}\times N^{\mathrm{R}}}$ is a unitary matrix and $\boldsymbol{\Lambda} \in \mathbb{R}^{N_r^{\mathrm{D}}\times N^{\mathrm{R}}}$ is a diagonal matrix with ordered eigenvalues $\lambda_1^{RD} > \lambda_2^{RD} > \cdots > \lambda_{r_{\min}}^{RD}$ along its main diagonal, which yields [25]

$$\begin{aligned} M_{\gamma^{SRD}\mid\boldsymbol{\Lambda}}(s) &= \frac{1}{\det\left(\boldsymbol{I}_{N_r^{\mathrm{D}}} - ((G^2\lambda_x\sigma_{SR}^2 s)/2N_0)\boldsymbol{\Lambda}\left(\boldsymbol{I}_{N_r^{\mathrm{D}}} + G^2\boldsymbol{\Lambda}\right)^{-1}\right)} \\ &= \prod_{n=1}^{r_{\min}}\left(\frac{1}{1-((G^2\lambda_x\sigma_{SR}^2 s\lambda_n^{RD})/(2N_0\left(1+G^2\lambda_n^{RD}\right)))}\right) \end{aligned} \tag{46}$$

where $r_{\min} = \min\{N^{\mathrm{R}}, N_r^{\mathrm{D}}\}$. The joint pdf of ordered eigenvalues is [26]

$$f_{\Lambda}(\lambda) = \frac{\prod_{n<m}^{r_{\min}}(\lambda_m-\lambda_n)^2\prod_{p=1}^{r_{\min}}\lambda_p^{r_{\max}-r_{\min}}\mathrm{e}^{-\lambda_p}}{\prod_{n=1}^{r_{\min}}\Gamma(r_{\max}-n+1)\Gamma(r_{\min}-n+1)} \tag{47}$$

where $r_{\max} = \max\{N^{\mathrm{R}}, N_r^{\mathrm{D}}\}$. The MGF of γ^{SRD} can be derived using (46) and (47) as (see (48)) . (48) can be calculated using Corollary 2 in [25] as

$$\begin{aligned} M_{\gamma^{SRD}}(s) = \mathscr{K}^{-1}\det\Bigg(\Bigg[\int_0^{\infty}&\left(1-\frac{G^2\lambda_x\sigma_{SR}^2 s\lambda_n^{RD}}{2N_0\left(1+G^2\lambda_n^{RD}\right)}\right)^{-1} \\ &\times\lambda^{(r_{\max}-r_{\min}+n+m-2)}\mathrm{e}^{-\lambda}\,\mathrm{d}\lambda\Bigg]_{n,m=1,\ldots,r_{\min}}\Bigg). \end{aligned} \tag{49}$$

where $\mathscr{K}^{-1} = \prod_{n=1}^{r_{\min}}\Gamma(r_{\max}-n+1)\Gamma(r_{\min}-n+1)$. Performing some algebraic manipulations in (49), the result in (35) can be obtained. This completes the derivation.

$$M_{\gamma^{SRD}}(s) = \int_{\lambda_1^{RD}}\cdots\int_{\lambda_{r_{\min}}^{RD}}\left(1-\frac{G^2\lambda_x\sigma_{SR}^2 s\lambda_n^{RD}}{2N_0\left(1+G^2\lambda_n^{RD}\right)}\right)^{-1} f_{\Lambda}(\lambda^{RD})\quad \mathrm{d}\lambda_1^{RD}\cdots\mathrm{d}\lambda_{r_{\min}}^{RD}. \tag{48}$$